

A dataset of floating debris accumulation at bridges after July 2021 flood in Germany and Belgium

Epicum, Sébastien; Poppema, Daan; Burghardt, Lisa; Benet, Loïc; Wüthrich, Davide; Klopries, Elena Maria; Dewals, Benjamin

DOI

[10.1038/s41597-024-03907-8](https://doi.org/10.1038/s41597-024-03907-8)

Publication date

2024

Document Version

Final published version

Published in

Scientific Data

Citation (APA)

Epicum, S., Poppema, D., Burghardt, L., Benet, L., Wüthrich, D., Klopries, E. M., & Dewals, B. (2024). A dataset of floating debris accumulation at bridges after July 2021 flood in Germany and Belgium. *Scientific Data*, 11(1), Article 1092. <https://doi.org/10.1038/s41597-024-03907-8>

Important note

To cite this publication, please use the final published version (if applicable). Please check the document version above.

Copyright

Other than for strictly personal use, it is not permitted to download, forward or distribute the text or part of it, without the consent of the author(s) and/or copyright holder(s), unless the work is under an open content license such as Creative Commons.

Takedown policy

Please contact us and provide details if you believe this document breaches copyrights. We will remove access to the work immediately and investigate your claim.



OPEN

DATA DESCRIPTOR

A dataset of floating debris accumulation at bridges after July 2021 flood in Germany and Belgium

Sébastien Ericpum¹✉, Daan Poppema², Lisa Burghardt³, Loïc Benet⁴, Davide Wüthrich², Elena-Maria Klopries³ & Benjamin Dewals¹

This paper presents a dataset documenting 71 floating debris accumulations at bridges following an extreme hydrological event that hit Belgium and Germany in July 2021. Data were collected from various sources including public authorities' documents, public online databases, post event pictures and field visits. The dataset covers bridges geometry, flood conditions and debris accumulation. In particular, it systematically details accumulations dimensions and quantifies accumulations components, which contain a significant portion of anthropogenic objects, in addition to driftwood. This dataset constitutes a unique set of invaluable data to better understand debris accumulation at bridges but also to analyze their impact on both the affected structures and flood conditions.

Background & Context

The study of floating objects transported by floods and the consequences of their possible accumulation at structures when they interact with the latter have gathered interest over the past decades.

Most of these works considered driftwood, i.e. tree trunks, eventually with roots bulb and branches^{1,2}. Such natural elements constitute indeed most of the floating debris observed during river floods. However, other objects, usually anthropogenic, can be transported by major floods, as recently shown by Bayon *et al.*³. They can be vehicles, furniture but also plastics or debris from damaged buildings for instance.

Heterogenous debris accumulations can behave differently than homogenous ones, leading to differing consequences at structures.

In the field of hydraulic structures engineering, events such as the one that occurred at Palagnedra dam in 1978 showed the risk to dam safety caused by driftwood accumulation⁴. Among others, Furlan *et al.*^{5,6} studied large wood blockage probability at spillways and Bénét *et al.*^{7,8} quantified the effect of driftwood accumulation at such dam safety structures and proposed solutions to mitigate it.

Several studies were related to driftwood accumulation at bridges, such as summarized by De Cicco *et al.*² and Schalko *et al.*⁹ for instance, or on solutions to block driftwood in rivers before they reach critical infrastructures¹⁰. Regarding bridge geometry, the effect of piers on blockage probability has received particular attention^{11,12} while only a few works focused on the deck and handrail^{13,14}.

In July 2021, an extreme flood hit Germany, Belgium, and The Netherlands, with several casualties and huge damages to household and infrastructures^{15,16}. Dozens of bridges were affected by blockage because of floating debris accumulation, with consequences on flood conditions and structural integrity^{17–19}. Shortly after the event, it became clear that observed debris accumulations at bridges, with substantial amounts of anthropogenic objects included in the debris, differed significantly from classic logjams made of trees. Observed accumulations composition shows similarities with the ones documented by Bayon *et al.*³ during urban flooding or with what can be observed during coastal flooding events (e.g. tsunamis, storm surges) where heterogeneous mixtures of floating debris are carried by the flow, accumulating at building and critical infrastructure^{20–22}.

The 2021 flood event, while dramatic, constituted a unique opportunity to collect invaluable field data on the geometry of bridges affected by debris accumulation and on the characteristics of these accumulations.

¹Liège Université, Liège, Belgium. ²Delft University of Technology, Delft, Netherlands. ³RWTH Aachen University, Aachen, Germany. ⁴SRP Ingénieur SA, Formerly Liège Université, Liège, Belgium. ✉e-mail: S.Ericpum@uliege.be

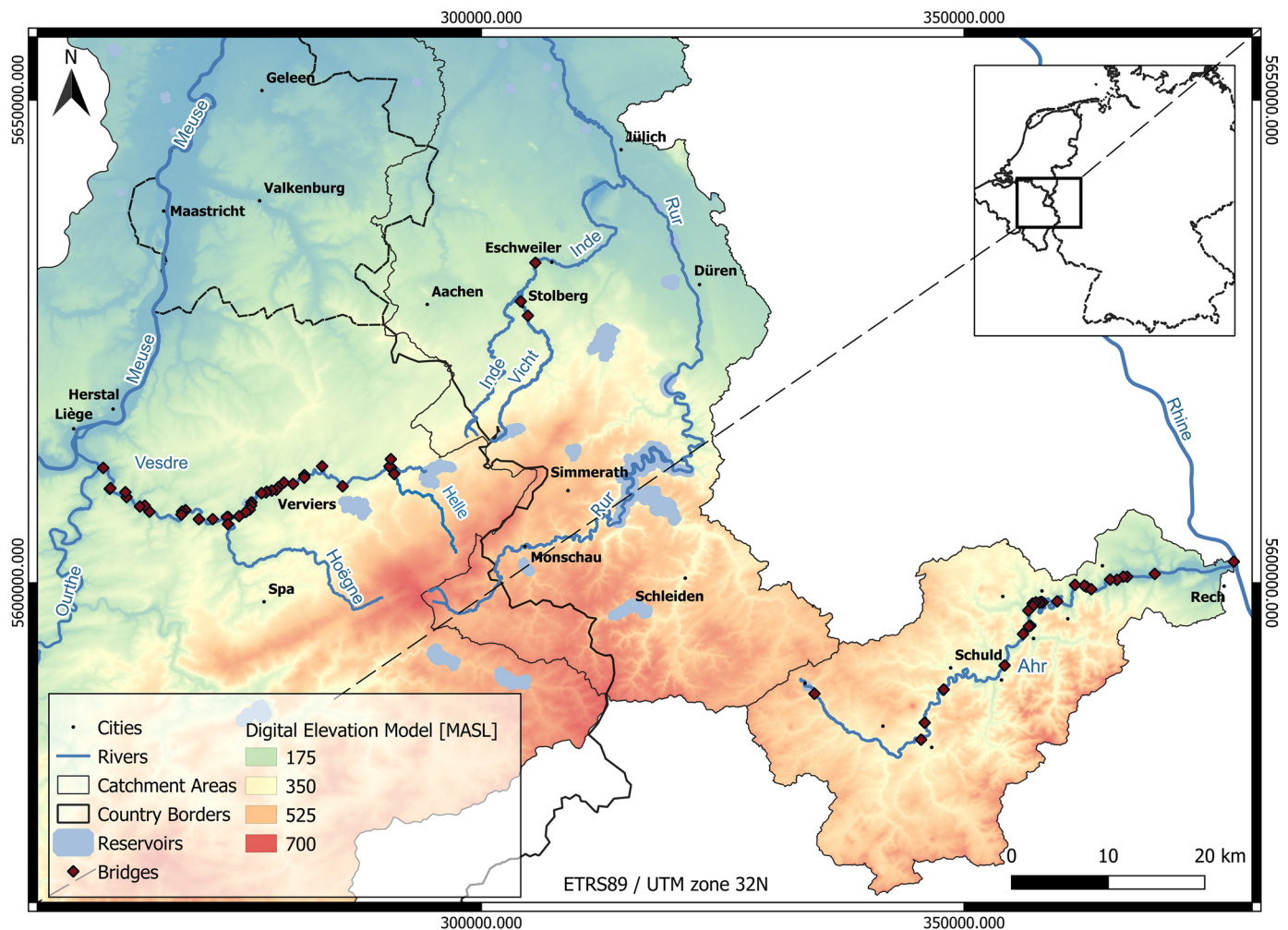


Fig. 1 Surveyed rivers and bridges with debris accumulations in Belgium and Germany³¹.

In this paper, we present a database systematically documenting bridges affected by floating debris accumulation during the July 2021 flood, the geometry of these accumulations and their composition. The data collection, performed by ULiege (Belgium), RWTH Aachen University (Germany) and TU Delft (The Netherlands) teams, covered six rivers particularly affected by the event in Belgium and Germany.

Method

Study area. The survey was performed along six of the most severely affected rivers during the July 2021 flood (Fig. 1), i.e. the Vesdre and its main tributaries the Helle and the Hoëgne in Belgium, and the Ahr, the Inde and the Vicht in Germany.

Except the Ahr River which is in the Rhine catchment, all these rivers are part of the Meuse catchment. They are relatively steep and small rivers, with average slope ranging from 0.5 to 1.7%, length from 23 to 86 km, and average discharge between 0.6 and 11 m³/s (Table 1). Their catchment areas, varying from 37 to 900 km², are largely dominated by natural areas (grassland, forest) upstream and the share of urban and industrial areas increases towards downstream, with for instance the Vesdre River crossing successively the towns of Eupen, Verviers and Chaudfontaine.

The upstream part of the Vesdre and the Vicht catchments is regulated by dam reservoirs while the other rivers are un-regulated.

Data sources and analysis. A total of 71 bridges affected by floating debris accumulation during the July 2021 flood event have been documented. These bridges are the ones passing over the six rivers considered in the study for which we have obtained pictures showing debris accumulation at the structures during or just after the flood. 38 bridges were located in Belgium, mainly on the Vesdre River, and 33 were located in Germany, mainly on the Ahr River (Fig. 1).

| River | Tributary of | Catchment area [km ²] | Average slope [%] | Length [km] | Average discharge [m ³ /s] | Estimated peak discharge during 2021 flood [m ³ /s] |
|--------|--------------|-----------------------------------|-------------------|-------------|---------------------------------------|--|
| Vesdre | Ourthe | 683 | 0.8 | 70 | 11 | 660 |
| Helle | Vesdre | 37 | 1.6 | 25 | 1.1 | 340 |
| Hoëgne | Vesdre | 200 | 1.7 | 30 | 3.5 | 265 |
| Ahr | Rhine | 900 | 0.5 | 86 | 7 | 800-1200 |
| Inde | Rur | 344 | 0.7 | 47 | 2.8 | n.a. |
| Vicht | Inde | 104 | 1.1 | 23 | 0.6 | >100 |

Table 1. Main characteristics of the surveyed rivers. Sources: for Vesdre, Helle and Hoëgne Rivers^{24–28}, for Ahr, Inde and Vicht Rivers^{29,30}, <https://wver.de/fluss/die-inde/>, <https://wver.de/fluss/die-vicht/>, <https://www.elwasweb.nrw.de/elwas-web/index.xhtml>, <https://www.hochwasser.rlp.de/flussgebiet/ahr/altenahr#pegelkennwerte>).

The data collection focused on the characteristics of the

- 1) Bridges: typology, location, geometry, degree of damage during the flood;
- 2) Debris accumulation at these bridges: geometry, composition;
- 3) Local hydraulic conditions during the flood: type of flow, peak discharge, water depth.

Regarding bridges, several sources of information were available and have been used to fill in the database. They are listed below by order of accuracy and easiness to access to the information, the first one being the most accurate and easiest to use to characterize a bridge geometry for instance.

- 1) Structural drawings received from the Landesbetrieb Mobilität Rheinland-Pfalz or Deutsche Bahn in Germany, and Service Public de Wallonie in Belgium;
- 2) Online cartographic portals (public administration portal) dedicated to the 2021 flood event with georeferenced maps and aerial photos for Germany (Flood 2021 platform by the German Federal Office of Civil Protection and Disaster Assistance - <https://arcgis.bbk.itzbund.de/arcgis/apps/sites/#/hochwasser2021>). WalOnMap platform in Belgium (<https://geoportail.wallonie.be/walonmap>) with georeferenced maps and aerial views allowing for elevations and bridges dimensions measurement;
- 3) *In situ* survey and measurements by members of the research teams if access to the structure was possible;
- 4) Post event pictures from local authorities, news agencies, inhabitants and social media.

Structural drawings have been used to define bridges geometry and elevations. When such drawings were not available or incomplete, data from the online cartographic portals and *in situ* measurements have been used. Bridges location has been defined from the online cartographic portals. Post event pictures have been mainly used to assess damages at the bridges during the flood.

When multiple sources of information were available, the first on the list were preferred to the next ones. In this respect, the most accurate and reliable source was always used for each parameter while limiting the time required to fill in the database.

Figure 2 shows an example of data used to characterize the geometry of bridge 30036 in Belgium.

Debris accumulations have mostly been characterized based on aerial and handheld photos taken during or just after the event. This is indeed the only available reliable source of information on the nature and geometry of the accumulations since these had quickly been removed and dismantled after the flood and were no longer present when the survey took place.

A total of 205 photos with visible debris accumulation, collected from local authorities, news agencies, inhabitants and social media, have been analyzed and processed. The software ImageJ (version 1.53) has been used to measure debris accumulations' lengths, heights and surfaces from pictures, using data from the bridge's geometry and surrounding structures for scale calibration (see Fig. 3 for an example for bridge 10016 in Germany). Information from different perspectives was combined to obtain both horizontal and vertical dimensions.

In order to maximize the accuracy of the estimations gained from pictures analysis, the following strategy has been applied. Three cases have been analyzed by three encoders from the three institutions part of the project. A first comparison of the results showed large variability (sometimes up to 200–300% variation in deposit volume evaluation for instance). The procedure has then been refined and a more stringent definition of the parameters has been discussed. This means that the list of parameters included in the database to characterize visible debris accumulations geometry and their definition above the water surface such as detailed in the following sections are the result of an iterative process performed during the project. Consequently, the variation in estimations of the parameters value by different encoders has been drastically reduced along iterations. In the following, each evaluation has been performed individually by two different researchers from the encoding institution. If both estimates varied less than 15%, the average value was encoded in the database. If they varied by 15% or more, estimations were performed again, and the results discussed between the encoders to get a value approved by both. This means 15% can be considered as an evaluation of the error range for the debris accumulation geometry parameters.

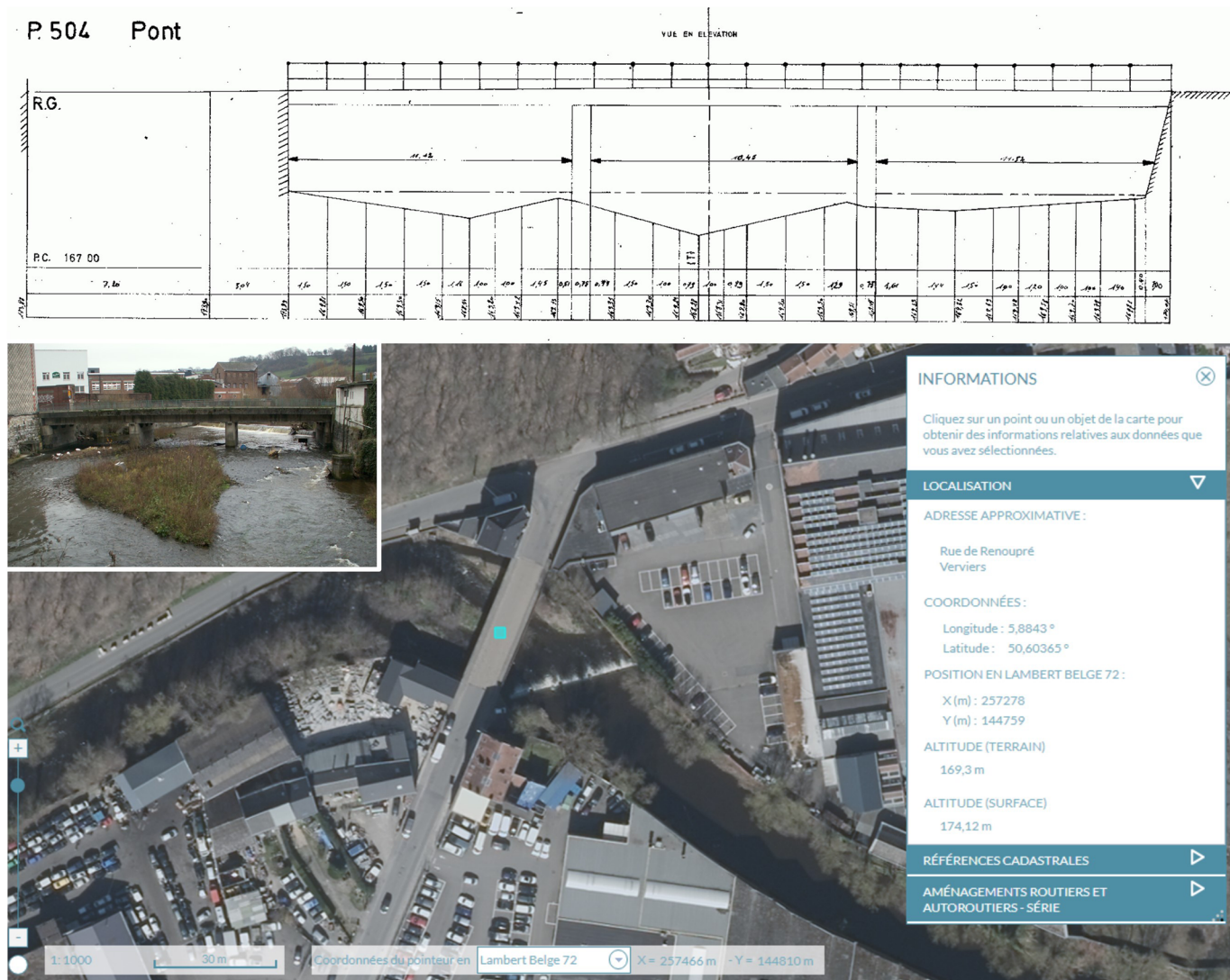


Fig. 2 Example of the data sources for bridge geometry characterization (bridge 30036 in the database, Verviers, Belgium). Structure drawings from public authorities (top), screenshot from the online cartographic portal WalOnMap (bottom) and picture from site visit (encapsulated).

Finally, data on flood conditions came from post-flood hydrological analysis²⁴ in Belgium; public authorities (LFU-RLP) in Germany) since most of the measurement stations located on the considered rivers have been damaged by the flood.

As a rule, in case of missing information, no value is mentioned in the database.

Data Records

The dataset is stored in a single CSV file, with semicolon separator, posted on Zenodo platform²³. The file contains 72 lines and 63 columns. First line contains the label of the columns. Each of the 71 following lines contains the data of one bridge and corresponding accumulation. The meaning of each label, i.e. the content of each column, and corresponding formatting and units, if required, is depicted in the Tables 2–7. In the following, labels have been grouped in 6 subgroups namely:

- 1) Identification (labels/columns 1 to 4)
- 2) Location (labels/columns 5 to 16)
- 3) Bridge geometry (labels/columns 17 to 36)
- 4) Flood conditions (labels/columns 37 to 42)
- 5) Accumulation properties (labels/columns 43 to 52)
- 6) Main debris content (labels/columns 53 to 63)



Result

$$W_{\text{tot}} = 36.1 \text{ m}$$

$$L_{\text{tot}} = 17.2 \text{ m} + 8.0 \text{ m} = 25.2 \text{ m}$$

$$H_{\text{tot}} = 4.7 \text{ m} + 1.0 \text{ m} = 5.7 \text{ m}$$

$$V_{\text{tot}} = 42 \text{ m}^2 \times 1\text{m} + 59 \text{ m}^2 \times 3\text{m} + 40 \text{ m}^2 \times 1.5\text{m} = 279 \text{ m}^3$$

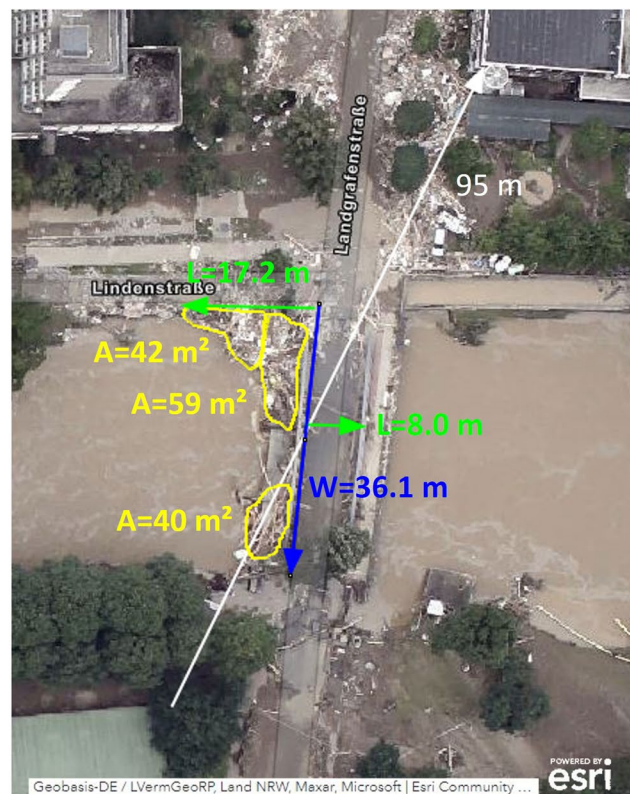


Fig. 3 Example of measurement of accumulation dimensions (W: width, L: length, H: height) and volume V, using photos from different perspectives (bridge 10016 in the database, Bad Neuenahr, Germany). Known dimensions of the bridge or surroundings are used for scale (indicated in white). Distances and areas directly measured on the photos are indicated in blue, green, magenta and yellow. The height of the three (yellow) areas is estimated rather than measured directly on the photo, given the lack of an undistorted straight-on perspective. Note the entanglement of debris with the bridge arch.

Identification. This group shows the unique identifier of the bridge in the database and identify by whom and when encoding has been done.

Location. This group contains the information needed to identify the structure and locate it.

Structure. This group contains a geometric description of the bridge.

Flood event at the structure. This group presents main flow conditions at the bridge during July 2021 event.

Accumulation. This group describes the debris accumulation blocked at the bridge.

Main debris content. This group presents the characteristics of the main elements constituting debris accumulation: percentage in volume and type of the maximum five elements constituting most of the accumulation.

Because of copyright issues related to the various sources of pictures, the latter are not publicly available in the database, but available on request.

Technical Validation

Double estimation of bridges and accumulation data, such as depicted in section *Data sources and analysis*, is the corner stone of data validation in this survey. It ensures that independent estimations of the same parameters exhibit a difference of less than 15%.

In addition, simple technical verifications have been performed after the dataset generation to verify its consistency. These concerned the bridges elevation and height values, length values, water depth and flow regime, and debris volumes. The following relations have been systematically verified:

- Center elevation of the bridge upper face (*Elevation*, Table 4) must be higher than the sum of the minimum elevation of the riverbed below the bridge (*Riverbed elevation*, Table 3) and the deck thickness at opening center (*Thickness*, Table 4);

| Label | Meaning | Values and formatting |
|-------------|---|-------------------------------------|
| ID | Five digits unique identifier of the bridge in the database | 10000 to 19999 → bridges in Germany |
| | | 30000 to 39999 → bridges in Belgium |
| Institution | Name of the institution responsible for the bridge encoding | RWTH or ULiège |
| Encoder | Initials of the researcher responsible for the encoding/final check | |
| Date | Date of encoding validation by the Encoder | [DD/MM/YYYY] |

Table 2. Parameters for identification.

| Label | Meaning | Values, formatting and units |
|-----------------------|---|--|
| Type | Type of structure | Bridge or Railway bridge |
| River | Name of the River on which the bridge has been erected | |
| Municipality | Name of the municipality where the bridge is situated | |
| Structure/street name | Name of the bridge or of the street passing over it | |
| EPSG | EPSG code of the coordinate reference system | Number between 1024 and 32767 |
| X reg | X coordinate of the bridge center in EPSG coordinate system | |
| Y reg | Y coordinate of the bridge center in EPSG coordinate system | |
| Lat | Latitude of the bridge center | [° N] |
| Long | Longitude of the bridge center | [° E] |
| Curv | Curvilinear abscissa of the bridge along river axis, counted from the river mouth | [m] |
| Riverbed elevation | Minimum elevation of the riverbed below the bridge | [m] |
| Upstream river shape | Shape of the riverbed upstream of the bridge | Straight: when a straight line directed upstream whose length is 5 times the river width and whose origin is on the center of the bridge upstream face does not cross a riverbank. |
| | | Curved right: when a straight line directed upstream whose length is 5 times the river width and whose origin is on the center of the bridge upstream face crosses the left riverbank. |
| | | Curved left: when a straight line directed upstream whose length is 5 times the river width and whose origin is on the center of the bridge upstream face crosses the right riverbank. |

Table 3. Parameters describing structure location.

- Horizontal dimension of the bridge deck from bank to bank (*Length*, Table 4) must be larger or equal to the sum of the number of pier(s) in the riverbed (*Number of piers*, Table 4) times the maximum dimension of the pier(s) perpendicular to riverbed axis (*Pier width*, Table 4) and the distance(s) between piers or abutments from left to right bank (*Distance between piers*, Table 4);
- Flow condition at the structure during the 2021 flood (*Type of flow*, Table 5) must be consistent with the maximum water elevation observed at the structure during the event (*Max water elevation*, Table 5), the bridge deck elevation (*Elevation*, Table 4) and the deck thickness (*Thickness*, Table 4);
- The total volume percentage of elements accumulated in debris deposit (sum of the 5 *Volume percentage* values in Table 7) must be lower or equal to 100%.

Data usage caution. Despite the systematic methodology applied to collect data, the reliability of estimations from pictures analysis is low and depends on post event pictures quality for each deposit, regardless of the encoding institution. It must be noted that accumulation dimensions are probably underestimated since they concern the visible part of the accumulation at the time of the survey. Given that water was flowing in the river, a part of the accumulation might be below the water surface and thus not visible. Also, as an effort to recover quickly after the flood, large debris accumulations at bridges were removed fast to restore river conveyance. Finally, the analysis is mostly based on post-event pictures and it is possible that the debris accumulation during the flood was larger than the one persisting after the event.

| Label | Meaning | Values and formatting |
|-------------------------------|---|---|
| <i>Opening(s) shape</i> | Shape of the opening(s) through which River flows | <i>Rectangular</i> or <i>Arched</i> |
| <i>Width</i> | Horizontal dimension of the bridge deck perpendicular to its length | [m] |
| <i>Length</i> | Horizontal dimension of the bridge deck from bank to bank | [m] |
| <i>Slope</i> | Slope of the bridge upper face, from right to left bank, positive in clockwise direction. | [%] |
| <i>Angle</i> | Angle between bridge width and left riverbank, positive in clockwise direction | [°] |
| <i>Thickness</i> | Deck thickness at opening center | [m] |
| <i>Elevation</i> | Center elevation of the bridge upper face | [m] |
| <i>River cross-section</i> | Shape of the river cross-section through the bridge | <i>Regular</i> : symmetric rectangular or trapezoidal cross section <i>Irregular</i> : any other cross section shape |
| <i>Abutments</i> | Abutment(s) on the riverbank | <i>Present</i> or <i>Absent</i> |
| <i>Number of piers</i> | Number of piers in the riverbed. Abutments are not considered as piers | |
| <i>Pier width</i> | Maximum dimension of the pier(s) perpendicular to riverbed axis | [m] |
| <i>Distance between piers</i> | Distance between piers or abutments from left to right bank | ... [m] (if a single opening is present, or all opening widths are identical) or ...-...-... [m] (if multiple openings present, number of piers + 1 values) |
| <i>Min distance</i> | Minimum distance between two adjacent piers or abutments | [m] |
| <i>Max distance</i> | Maximum distance between two adjacent piers or abutments | [m] |
| <i>Pier shape</i> | Shape of pier nose facing the flow | <i>Circular</i> : circular pier <i>Rounded</i> : rounded nose <i>Sharp</i> : triangular nose <i>Square</i> : flat nose (no profiling) <i>No pier</i> : no piers present |
| <i>Pier protrusion</i> | Distance between the pier upstream nose and the bridge deck | [m] |
| <i>Handrail material</i> | Material of the handrail | <i>Stone, metal, mixed</i> (stone and metal) or <i>other</i> |
| <i>Handrail height</i> | Height of the handrail | [m] |
| <i>Handrail porosity</i> | Estimated ratio of openings area to solid area in handrail | <i>Total</i> : no handrail <i>High</i> : handrail made of thin elements with large spacing <i>Medium</i> : handrail made of thin elements with low spacing <i>Low</i> : handrail made of broad elements with low spacing <i>No porosity</i> : continuous wall |
| <i>Structure damage</i> | Level of damage to the bridge observed after July 2021 event | <i>No</i> : no damage <i>Weak</i> : small and limited extent damage without compromising bridge use and stability <i>Moderate</i> : local damage at several spots without compromising bridge use and stability <i>Strong</i> : damage preventing use of the structure but not compromising stability <i>Complete</i> : the structure is no more present, or integrity is compromised |

Table 4. Parameters describing bridge geometry.

| Label | Meaning | Values and formatting |
|----------------------------|---|---|
| <i>Flood event</i> | Name of flood event | |
| <i>Type of flow</i> | Flow condition at the structure | <i>Free surface</i> : the peak water level is below the bridge deck <i>Pressurized</i> : the peak water level is between the bottom and top of the bridge deck <i>Mixed</i> : the peak water level is above the bridge deck |
| <i>Discharge</i> | Max flow discharge in the river at the structure location during the event | [m ³ /s] |
| <i>Max water elevation</i> | Maximum water elevation observed at the structure during the event | [m] |
| <i>Max water depth</i> | Difference between <i>max water elevation</i> and <i>riverbed elevation</i> | [m] |
| <i>Flow width</i> | Flow width at the structure location during the event | [m] |

Table 5. Parameters describing flood conditions at structure location.

| Label | Meaning | Values and formatting |
|------------------------------|--|---|
| <i>Clogging</i> | Debris accumulation at the bridge opening during the event, resulting in bridge clogging | Yes: yes with certainty |
| | | No: no with certainty |
| | | No information: not clear based on available information, signs of accumulations may be visible (single locks stuck at the railing) but no certain information about an accumulation can be drawn (and would only be an assumption) |
| <i>Carpet</i> | Continuous and compact accumulation of debris just upstream of the bridge | Yes: yes with certainty |
| | | No: no with certainty |
| | | No information: not clear based on available information |
| <i>Total length</i> | Max. dimension parallel to river axis of debris accumulation area upstream of the bridge | [m] |
| <i>Total width</i> | Max. dimension normal to river axis of debris accumulation area upstream of the bridge | [m] |
| <i>Total height</i> | Max. visible vertical dimension of debris accumulation area upstream of the bridge | [m] |
| <i>Carpet length</i> | Max. dimension of the carpet parallel to river axis | [m] |
| <i>Carpet width</i> | Max. dimension of the carpet normal to river axis | [m] |
| <i>Carpet height</i> | Max. visible vertical dimension of the carpet | [m] |
| <i>Volume</i> | Visible volume of debris blocked at the bridge | [m ³] |
| <i>Location at structure</i> | Location of the debris at the bridge | <i>Whole width</i> : debris accumulation occupies at least 80% of the bridge length |
| | | <i>Right bank</i> : debris accumulation is less than 80% of the bridge length and is mainly on right bank of the bridge |
| | | <i>Left bank</i> : debris accumulation is less than 80% of the bridge length and is mainly on left bank of the bridge |
| | | <i>Center</i> : debris accumulation is less than 80% of the bridge length and is centered at the bridge |
| | | <i>Pier(s)</i> : debris accumulation is limited and only at pier(s) |
| | | <i>Handrail</i> : debris accumulation is only at handrail |

Table 6. Parameters describing the deposit blocked at the bridge.

| Label | Meaning | Values and formatting |
|----------------------------|--|--|
| <i>Main trunk presence</i> | Presence of a large trunk (compare to structure opening) blocked in bridge opening | Yes: yes with certainty |
| | | No: no with certainty |
| | | No information: not clear based on available information |
| <i>Id main type i</i> | Type of elements (<i>i</i> from 1 to 5) | 20: Natural wood |
| | | 21: Anthropogenic wood |
| | | 22: Plastic container |
| | | 23: Metal container |
| | | 24: Vehicle |
| | | 25: Household items |
| | | 26: Industry items |
| <i>Volume percentage i</i> | Volume in percent of elements of <i>main type i</i> compared to <i>Volume</i> | 27: Building rubble |
| | | 30: Other |
| | | [%] |

Table 7. Parameters describing the debris constituting the deposit blocked at the bridge.

Usage Notes

This dataset is intended to provide field data about bridges affected by floating debris blockage during an extreme flood event and corresponding debris accumulation properties. It details 71 bridges and accumulations, mainly on the Vesdre and Ahr Rivers in Belgium and Germany, with more than 60 parameters per case. This dataset is expected to be valuable since it systematically details real floating debris and accumulations observed following a rare hydrological event that took place in Western Europe in July 2021. It is therefore a unique image of a natural hazard for which our societies are trying to protect themselves.

Code availability

No custom code has been used in this study. The software ImageJ (<https://imagej.net/ij/>), version 1.53, has been used to extract dimensions from debris accumulations' pictures.

Received: 13 June 2024; Accepted: 19 September 2024;

Published online: 05 October 2024

References

- Comiti, F., Lucía, A. & Rickenmann, D. Large wood recruitment and transport during large floods: a review. *Geomorphology* **269**, 23–39 (2016).
- De Cicco, P. N., Paris, E., Ruiz-Villanueva, V., Solari, L. & Stoffel, M. In-channel wood-related hazards at bridges: A review. *River Research and Applications* **34**(7), 617–628, <https://doi.org/10.1002/rra.3300> (2018).
- Bayón, A., Valero, D. & Franca, M. J. Urban Flood Drifters (UFDs): identification, classification and characterisation. *J. of Flood Risk Management* **2024**, e13002, <https://doi.org/10.1111/jfr3.13002> (2024).
- Bruschin, J., Bauer, S., Delley, P. & Trucco, G. The overtopping of the Palagnedra dam. *Water Power Dam Constr.* **34**(1), 13–19 (1981).
- Furlan, P., Pfister, M., Matos, J., Amado, C. & Schleiss, A. J. Experimental repetitions and blockage of large stems at ogee crested spillways with piers. *J. Hyd. Res.* **57**(2), 250–262, <https://doi.org/10.1080/00221686.2018.1478897> (2018).
- Furlan, P., Pfister, M., Matos, J., Amado, C., Schleiss, A. J. Blockage probability modeling of large wood at reservoir spillways with piers. *Wat. Res. Res.*, 57(8). <https://doi.org/10.1029/2021WR029722> (2021).
- Bénet, L., De Cesare, G. & Pfister, M. Reservoir Level Rise under Extreme Driftwood Blockage at Ogee Crest. *J. Hyd. Eng.* **147**(1). [https://doi.org/10.1061/\(ASCE\)HY.1943-7900.0001818](https://doi.org/10.1061/(ASCE)HY.1943-7900.0001818) (2020).
- Bénet, L., De Cesare, G. & Pfister, M. Partial Driftwood Rack at Gated Ogee Crest: Trapping Rate and Discharge Efficiency. *J. Hyd. Eng.* **148**(8). [https://doi.org/10.1061/\(ASCE\)HY.1943-7900.0001994](https://doi.org/10.1061/(ASCE)HY.1943-7900.0001994) (2022).
- Schalcko, I., Lageder, C., Schmocker, L., Weitbrecht, V. & Boes, R. M. Laboratory flume experiments on the formation of spanwise large wood accumulations: I. Effect on backwater rise. *Wat. Res. Res.* **55**(6), 4854–4870, <https://doi.org/10.1029/2018WR024649> (2019).
- Schalcko, I., Schmocker, L., Weitbrecht, V. & Boes, R. M. Risk reduction measures of large wood accumulations at bridges. *Env. Fluid Mech.* **20**(3), 485–502, <https://doi.org/10.1007/s10652-019-09719-4> (2020a).
- De Cicco, P. N., Paris, E., Solari, L. & Ruiz-Villanueva, V. Bridge pier shape influence on wood accumulation: Outcomes from flume experiments and numerical modelling. *J. of Flood Risk Management* **13**(2), e12599 (2020).
- Schalcko, I., Schmocker, L., Weitbrecht, V. & Boes, R. M. Laboratory study on wood accumulation probability at bridge piers. *J. Hyd. Res.* **58**(4), 566–581, <https://doi.org/10.1080/00221686.2019.1625820> (2020b).
- Schmocker, L. & Hager, W. H. Probability of Drift Blockage at Bridge Decks. *J. Hyd. Eng.* **137**(4), 470–479, [https://doi.org/10.1061/\(ASCE\)HY.1943-7900.0000319](https://doi.org/10.1061/(ASCE)HY.1943-7900.0000319) (2011).
- Gschnitzer, T., Gems, B., Mazzorana, B. & Aufleger, M. Towards a robust assessment of bridge clogging processes in flood risk management. *Geomorphology* **279**, 128–140, <https://doi.org/10.1016/j.geomorph.2016.11.002> (2017).
- Mohr, S. *et al.* A multi-disciplinary analysis of the exceptional flood event of July 2021 in central Europe – Part 1: Event description and analysis. *Natural Hazards and Earth System Sciences* **23**(2), 525–551, <https://doi.org/10.5194/nhess-23-525-2023> (2023).
- Koks, E. E., van Ginkel, K. C. H., van Marle, M. J. E. & Lemnitzer, A. Brief communication: Critical infrastructure impacts of the 2021 mid-July western European flood event. *Natural Hazards and Earth System Sciences* **22**(12), 3831–3838, <https://doi.org/10.5194/nhess-22-3831-2022> (2022).
- Burghardt, L., Klopries, E.-M., & Schüttrumpf, H. Structural damage, clogging, collapsing: Analysis of the bridge damage at the rivers Ahr, Inde and Vicht caused by the flood of 2021. *Journal of Flood Risk Management*, e13001. <https://doi.org/10.1111/jfr3.13001> (2024).
- Tubaldi, E. *et al.* Invited perspectives: Challenges and future directions in improving bridge flood resilience. *Natural Hazards and Earth System Sciences* **22**(3), 795–812, <https://doi.org/10.5194/nhess-22-795-2022> (2022).
- Wüthrich, D. *et al.* Field survey assessment of flood loads and related building damage from the July 2021 event in the Ahr Valley (Germany). *Journal of Flood Risk Management*, e13024, <https://doi.org/10.1111/jfr3.13024> (2024).
- Robertson, I. N., Riggs, H. R., Yim, S. C. & Young, Y. L. Lessons from Hurricane Katrina Storm Surge on Bridges and Buildings. *Journal of Waterway, Port, Coastal, and Ocean Engineering* **133**(6), 463–483, [https://doi.org/10.1061/\(ASCE\)0733-950X\(2007\)133:6\(463\)](https://doi.org/10.1061/(ASCE)0733-950X(2007)133:6(463)) (2007).
- Chock, G., Robertson, I., Kriebel, D., Francis, M., & Nistor, I. *Tohoku, Japan, earthquake and tsunami of 2011: Performance of structures under tsunami loads*. ASCE Report (2013).
- Wüthrich, D., Arbós, C. Y., Pfister, M. & Schleiss, A. J. Effect of Debris Damming on Wave-Induced Hydrodynamic Loads against Free-Standing Buildings with Openings. *Journal of Waterway, Port, Coastal, and Ocean Engineering* **146**(1), 04019036, [https://doi.org/10.1061/\(ASCE\)WW.1943-5460.0000541](https://doi.org/10.1061/(ASCE)WW.1943-5460.0000541) (2020).
- Erpicum, S. *et al.* Database - Bridge clogging and debris - July 2021 flood (1.0). *Zenodo*. <https://doi.org/10.5281/zenodo.11551195> (2024).
- Dessers, C., Archambeau, P., Dewals, B., Erpicum, S. & Piroton, M. Hydrological modelling of July 2021 floods in Vesdre and Amblève catchments, *EGU General Assembly 2023*, Vienna, Austria, 24–28 Apr 2023, EGU23-15619, <https://doi.org/10.5194/egusphere-egu23-15619> (2023).
- Bauwens, A., Sohier, C. & Degré, A. Hydrological response to climate change in the Lesse and the Vesdre catchments: contribution of a physically based model (Wallonia, Belgium). *Hydrol. Earth Syst. Sci.* **15**(6), 1745–1756, <https://doi.org/10.5194/hess-15-1745-2011> (2011).
- Bruwier, M., Erpicum, S., Piroton, M., Archambeau, P. & Dewals, B. J. Assessing the operation rules of a reservoir system based on a detailed modelling chain. *Nat. Hazards Earth Syst. Sci.* **15**(3), 365–379, <https://doi.org/10.5194/nhess-15-365-2015> (2015).
- Cuvelier, T., Archambeau, P., Dewals, B. & Louveaux, Q. Comparison Between Robust and Stochastic Optimisation for Long-term Reservoir Management Under Uncertainty. *Water Resources Management* **32**(5), 1599–1614, <https://doi.org/10.1007/s11269-017-1893-1> (2018).
- Deroanne, C., & Petit, F. Longitudinal evaluation of the bed load size and of its mobilisation in a gravel bed river. *Floods and Landslides: Integrated Risk Assessment* (pp. 335–342). Springer (1999).
- Roggenkamp, T. & Herget, J. Hochwasser der Ahr im Juli 2021 – Abflussabschätzung und Einordnung. *Hydrologie und Wasserbewirtschaftung* **66**(1), 40–49 (2022).
- Vorogushyn, S., Apel, H., Kemter, M. & Thieken, A. H. Analyse der Hochwassergefährdung im Ahrtal unter Berücksichtigung historischer Hochwasser. *Hydrologie und Wasserbewirtschaftung* **66**(5), 244–254, https://doi.org/10.5675/HyWa_2021.5_2 (2022).
- OpenStreetMap contributors. *Planet dump*. Retrieved from <https://planet.openstreetmap.org> (2015).

Acknowledgements

This research was carried out within the context of Interreg project EMfloodResilience, project no. 228, co-funded by the European Regional Development Fund. The Authors thank Florence Dütz, Gianni Massin, Mariana Vélez Pérez, Lino Schröter, and Mariia Gimelbrant for their assistance in the photo analysis and data collection. Figure 1 map data copyrighted OpenStreetMap contributors and available from <https://www.openstreetmap.org>.

Author contributions

Daan Poppema, Lisa Burghardt, Loïc Benet: methodology, data collection, data quality control, writing; Sébastien Erpicum, Davide Wüthrich, Elena-Maria Klopries, Benjamin Dewals: conceptualization, funding, project administration, supervision; Sébastien Erpicum: data quality control, writing; All authors have contributed to reviewing the manuscript.

Competing interests

The authors declare no competing interests.

Additional information

Correspondence and requests for materials should be addressed to S.E.

Reprints and permissions information is available at www.nature.com/reprints.

Publisher's note Springer Nature remains neutral with regard to jurisdictional claims in published maps and institutional affiliations.



Open Access This article is licensed under a Creative Commons Attribution-NonCommercial-NoDerivatives 4.0 International License, which permits any non-commercial use, sharing, distribution and reproduction in any medium or format, as long as you give appropriate credit to the original author(s) and the source, provide a link to the Creative Commons licence, and indicate if you modified the licensed material. You do not have permission under this licence to share adapted material derived from this article or parts of it. The images or other third party material in this article are included in the article's Creative Commons licence, unless indicated otherwise in a credit line to the material. If material is not included in the article's Creative Commons licence and your intended use is not permitted by statutory regulation or exceeds the permitted use, you will need to obtain permission directly from the copyright holder. To view a copy of this licence, visit <http://creativecommons.org/licenses/by-nc-nd/4.0/>.

© The Author(s) 2024